

Air Force Institute of Technology

AFIT Scholar

Faculty Publications

12-24-2007

An Explanation of SRS Beam Cleanup in Graded-index Fibers and the Absence of SRS Beam Cleanup in Step-index Fibers

Nathan B. Terry

Air Force Research Laboratory


Thomas G. Alley

Lockheed Martin

Timothy H. Russell

Air Force Institute of Technology

Follow this and additional works at: <https://scholar.afit.edu/facpub>

 Part of the [Plasma and Beam Physics Commons](#), and the [Semiconductor and Optical Materials Commons](#)

Recommended Citation

Terry, Nathan B.; Alley, Thomas G.; and Russell, Timothy H., "An Explanation of SRS Beam Cleanup in Graded-index Fibers and the Absence of SRS Beam Cleanup in Step-index Fibers" (2007). *Faculty Publications*. 217.

<https://scholar.afit.edu/facpub/217>

This Article is brought to you for free and open access by AFIT Scholar. It has been accepted for inclusion in Faculty Publications by an authorized administrator of AFIT Scholar. For more information, please contact richard.mansfield@afit.edu.

An explanation of SRS beam cleanup in graded-index fibers and the absence of SRS beam cleanup in step-index fibers

Nathan B. Terry^{1,2*}, Thomas G. Alley^{1,3}, Timothy H. Russell¹

¹Air Force Institute of Technology, 2950 Hobson Way, Wright-Patterson Air Force Base, OH 45433

²Current address: Air Force Research Laboratory, 2241 Avionics Circle,
Wright-Patterson Air Force Base, OH 45433

³Current address: Lockheed Martin Coherent Technologies, 135 South Taylor Av,
Louisville, CO 80027

*Corresponding author: nathan.terry@wpafb.af.mil

Abstract: Beam cleanup via stimulated Raman scattering in multimode fibers is modeled by numerically considering the competition between the Stokes modes of graded-index and step-index fibers. The relative gain of each Stokes mode is calculated by considering the overlap the various pump and Stokes modes of the fibers. Mode competition in a graded-index fiber favors the LP_{01} Stokes mode while mode competition in a step-index fiber does not favor the LP_{01} Stokes mode. This model explains why beam cleanup has only been reported for graded-index fibers and not for step-index fibers.

©2007 Optical Society of America

OCIS codes: (060.2320) Fiber Optics, Oscillators and Amplifiers; (190.4370) Nonlinear Optics, Fibers; (290.5910) SRS; (999.9999) Multimode Fibers; (999.9999) Graded-Index Fibers; (999.9999) Step-Index Fibers.

References and links

1. K. S. Chiang, "Stimulated Raman scattering in a multimode optical fiber: evolution of modes in Stokes waves," *Opt. Lett.* **17**, 352 (1992).
2. T. H. Russell, S. M. Willis, M. B. Crookston and W. B. Roh, "Stimulated Raman scattering in multimode fibers and its application to beam cleanup and combining," *J. Nonlinear Opt. Phys. Mater.* **11**, 303-316 (2002).
3. P. L. Baldeck, F. Raccach and R. R. Alfano, "Observation of self-focusing in optical fibers with picosecond pulses," *Opt. Lett.* **12**, 588 (1987).
4. Z. V. Nesterova, I. V. Aleksandrov, A. A. Polnitskii, D. K. Sattarov, "Propagation characteristics of high power ultrashort light pulses in optical fibers," *JETP Lett.* **34**, 371 (1981).
5. B. M. Flusche, T. G. Alley, T. H. Russell, and W. B. Roh, "Multi-port beam combination and cleanup in large multimode fiber using stimulated Raman scattering," *Opt. Express* **14**, 11748, (2006).
6. T.Y. Fan, "Laser beam combining for high-power, high-radiance sources," *IEEE J. Sel. Top. Quantum Electron.* **11**, 567-577 (2005).
7. S. H. Baek and W. B. Roh, "Single-mode Raman fiber laser based on a multimode fiber," *Opt. Lett.* **29**, 153 (2004).
8. N. B. Terry, K. T. Engel, T. G. Alley, and T. H. Russell, "Use of a continuous wave Raman fiber laser in graded-index multimode fiber for SRS beam combination," *Opt. Express* **15**, 602-7 (2007).
9. A. Polley and S. E. Ralph, "Raman amplification in multimode Fiber," *IEEE Photon. Technol. Lett.* **19**, 218 (2007).
10. M. D. Sharma, Z. Q. Wu, R. Posey, A. Williams, P. Venkateswarlu, "Stimulated Raman scattering in a multimode optical fiber with bend-induced loss," *Opt. Commun.* **111**, 127 (1994).
11. R. G. Smith, "Optical power handling capacity of low loss optical fibers as determined by stimulated Raman and Brillouin scattering," *Appl. Opt.* **11**, 2490 (1972).
12. G. P. Agrawal, *Nonlinear Fiber Optics*, 3rd ed., (Academic Press, San Diego, 2001), Chap. 8.
13. R. H. Stolen, "Fiber Raman lasers," *Fiber and Integr. Opt.* **3**, 21-51 (1980).
14. E. M. Dianov, I. A. Bufetov, M. M. Bubnov, M. V. Grekov, S. A. Sasiliev, O. I. Medvedkov, A. V. Shubin, A. N. Guryanov, V. F. Khopin, M. V. Yashkov, E. M. Deliso, D. L. Butler, "1.3 μm Raman fiber amplifier," *Proc. SPIE* **4083**, 101-109, (2000).

15. T. H. Russell, B. W. Grime, T. G. Alley and W. B. Roh, "Stimulated Brillouin scattering beam cleanup and Combining in optical Fiber", to be published in *Nonlinear Optics and Recent Advances in Optics*, Research Signpost (2007).
16. A. W. Snyder, J. D. Love, *Optical Waveguide Theory*, (Chapman and Hall, New York, 1983).
17. B. E. A. Saleh, M. C. Teich, *Fundamentals of Photonics*, (John Wiley and Sons, New York, 1991), Chap. 8.

1. Introduction

Stimulated Raman scattering (SRS), a non-linear optical process whereby a pump photon is converted to a longer wavelength Stokes photon, has long been recognized as method of generating novel wavelengths. SRS possesses an interesting property of beam cleanup such that a multimode pump beam generates a Stokes beam with good beam quality. This property has been demonstrated in fibers [1-5] and bulk media [6]. SRS fiber beam cleanup allows Raman fiber lasers pumped with multimode pump lasers to produce Stokes beams with good beam quality [7]. SRS beam cleanup can also be used for highly efficient SRS beam combination in fiber [8], as well as multimode fiber communication links [9]. These applications however, require the use of a graded-index fiber; SRS beam cleanup has not been observed in step-index fibers [9,10]. To the best of our knowledge there is no reported model that explains why beam cleanup does not occur in step-index fibers.

In this paper, we present a model which explains why step-index fibers are unsuitable for SRS fiber beam cleanup. Section 2 contains a derivation of an equation for the gain of each of the Stokes modes of a multimode fiber in terms of the mode distribution of the input pump beam. In section 3, we use this gain equation to calculate the relative gain of the Stokes modes of both a graded-index and a step-index fiber. The relative gain of the fiber modes is used to explain SRS beam cleanup in a graded-index fiber; the relative gain is also used to describe the absence of beam cleanup in a step-index fiber. Section 4 of this paper explores the consequences of these formulas by presenting graphical examples of beam cleanup in a graded-index fiber and the lack of beam cleanup in a step-index fiber. Animations of the evolution of the Stokes modes are also included. This paper concludes with a discussion of our results.

2. Raman gain of individual fiber modes

In the case of unseeded SRS generation, the initial Stokes beam arises from the amplification of Stokes photons generated by spontaneous Raman scattering. In a long fiber ($\alpha_p L \gg 1$), where α_p is the attenuation of the pump beam and L is the length of the fiber, spontaneous Raman scattering can be viewed as seeding by one fictitious photon per transverse and longitudinal mode of the fiber [11]. The model of unseeded SRS beam cleanup in a long fiber presented here considers the initial power in the Stokes beam to be uniformly distributed between the transverse modes of the fiber. Furthermore, we assume that the Stokes power is confined to a single longitudinal mode; the pump power is likewise considered to be confined to a single longitudinal mode.

Given a uniform initial mode distribution of Stokes power in a long fiber, we now consider how the power in the Stokes power modes is amplified by the pump beam. The interaction of the pump beam with the Stokes beam in SRS is described by [12]

$$\begin{aligned} \frac{dI_p(r, \theta, z, t)}{dz} &= -\frac{\omega_p}{\omega_s} g_R I_p(r, \theta, z, t) I_s(r, \theta, z, t) - \alpha_p I_p(r, \theta, z, t) \\ \frac{dI_s(r, \theta, z, t)}{dz} &= g_R I_p(r, \theta, z, t) I_s(r, \theta, z, t) - \alpha_s I_s(r, \theta, z, t) \end{aligned} \quad (1)$$

In this set of equations, I is the irradiance of the beam, ω is the frequency and α is the attenuation, with the subscripts p and s denoting the pump and Stokes components respectively. The Raman gain coefficient is denoted by g_R . While not critical to this

derivation, the time dependence is included for completeness. To convert these equations into a form relating the power in the pump beam to the power in the Stokes beam, the intensity equations are integrated over the area of the fiber. In terms of power, the coupled differential equations then take on the following form

$$\begin{aligned}\frac{dP_p(z,t)}{dz} &= -g(z,t)\frac{\omega_p}{\omega_s}P_p(z,t)P_s(z,t) - \alpha_p P_p(z,t) \\ \frac{dP_s(z,t)}{dz} &= g(z,t)P_p(z,t)P_s(z,t) - \alpha_s P_s(z,t)\end{aligned}\quad (2)$$

where P represents power. The Raman gain, $g(z)$, is expressed in terms of the overlap of the pump beams and the Stokes beams according to

$$g(z,t) = g_R \frac{\iint I_p(r,\theta,z,t)I_s(r,\theta,z,t)rdrd\theta}{P_p(z)P_s(z)} \quad (3)$$

The overlap integral of Eq. (3) has been considered by previous authors. For example, Stolen introduced the overlap integral as a method of computing the Raman gain of Raman fiber lasers [13]. Dianov *et al.* considered this integral in their analysis of a Raman fiber amplifier based on a singlemode fiber [14]. Russell *et al.* used the overlap integral to analyze unseeded beam cleanup via stimulated Brillouin scattering [15]. Polley and Ralph used this overlap integral to show that the gain of the LP_{01} mode of a graded-index fiber was comparable to the gain of a standard singlemode fiber [9].

Chiang considered the overlap integral in his analysis of SRS beam cleanup in multimode fibers [1]. However, Chiang calculated the overlap integrals of a step-index fiber and applied them to a graded-index fiber. Furthermore, Chiang only considered SRS fiber beam cleanup for a single carefully chosen launching condition of the pump beam. The model of SRS beam cleanup presented here describes beam cleanup in graded-index and step-index fibers in terms of their respective overlap integrals for a range of launching conditions.

The intensity terms of the overlap integral of Eq. (3) are related to the electric fields of the fiber modes by

$$I_{p,s}(r,\theta,z,t) = 2\varepsilon_0 c n_{p,s}(r) \left\langle \left| \bar{E}_{p,s}(r,\theta,z,t) \right|^2 \right\rangle \quad (4)$$

where ε_0 is the electric permeability of vacuum, c is the speed of light and n is the index of refraction of the fiber and $\bar{E}_{p,s}$ represents the electric field of the pump and Stokes modes. The brackets denote the time average. The electric field in a multimode fiber can be considered to be a superposition of fiber modes according to

$$\bar{E}_{p,s}(r,\theta,z,t) = \sum_q A_{p,s}^q \psi_{p,s}^q(r,\theta) [\cos(\bar{k}_{p,s}^q \cdot \hat{z} - \omega_{p,s}t + \phi_{p,s}^q)] \hat{e}_{p,s}, \quad (5)$$

where $A_{p,s}^q$ is the amplitude, $\psi_{p,s}^q$ is the mode field, $\phi_{p,s}^q$ is the phase, and $\bar{k}_{p,s}^q$ is wavevector of the q^{th} mode of the fiber. The frequency is represented by $\omega_{p,s}$; \hat{e} is a unit vector.

The fields of the LP_{lm} modes of a weakly-guiding graded-index fiber are given by [16]

$$\psi_{lm} = \cos(l\phi) R^l L_{m-1}^{(l)}(VR^2) \exp\left(-\frac{1}{2} VR^2\right), \quad (6)$$

where $L_{m-1}^{(l)}$ represents the associated Laguerre polynomial; $R=r/a$, where a is the radius of the fiber. The radial and the azimuthal coordinates of the fiber are represented by r and θ respectively. The LP_{lm} modes of a weakly-guiding step-index fiber are given by [16, 17]

$$\psi_{lm} = \frac{J_l(U_{lm}R)}{J_{l-1}(U_{lm})} \cos(l\theta), \quad (7)$$

where J_l is the Bessel function of the l^{th} order and k_{lm} is the wave number of associated with the LP_{lm} mode. U_{lm} is the solution of the following characteristic equation

$$U_{lm} \frac{J_{l+1}(U_{lm})}{J_l(U_{lm})} = W_{lm} \frac{K_{l+1}(W_{lm})}{K_l(W_{lm})}, \quad (8)$$

and where $U_{lm}^2 + W_{lm}^2 = V^2$.

By incorporating Eq. (4) and Eq. (5) into Eq. (3), the total Raman gain of the fiber is given by

$$g(z) = g_R [\varepsilon_0 \text{cn}(r)]^2 \frac{\sum_j A_s^j \sum_v A_s^v \sum_m A_p^m \sum_q A_p^q \gamma^{jvmq}}{P_s(z) P_p(z)}, \quad (9)$$

where

$$\gamma^{jvmq} = \int_0^a \int_0^{2\pi} [\psi_s^j \psi_s^v \psi_p^m \psi_p^q \cos(\Delta \bar{k}_s^{jv} \cdot \hat{z} + \Delta \varphi_s^{jv}) \times \cos(\Delta \bar{k}_p^{mq} \cdot \hat{z} + \Delta \varphi_p^{mq})] r dr d\theta. \quad (10)$$

and

$$\begin{aligned} \Delta \bar{k}_{p,s}^{nl} &\equiv \bar{k}_{p,s}^n - \bar{k}_{p,s}^l \\ \Delta \varphi_{p,s}^{nl} &\equiv \varphi_{p,s}^n - \varphi_{p,s}^l \end{aligned} \quad (11)$$

Equation (9) describes the total Raman gain of the fiber. A quantitative analysis of mode competition however, requires a description of the gain of the individual modes of the fiber. An approximate description of the gain of the individual modes can be obtained by considering the individual gain terms comprising Eq. (9). The following convention will be used to simplify the notation

$$A_s^j A_s^v A_p^m A_p^q \gamma^{jvmq} \equiv g_{jvmq}, \quad (12)$$

where j and v correspond to the Stokes beam; m and q correspond to the pump beam. For the simple case of a fiber with only two transverse pump modes and two transverse Stokes modes, the terms comprising the total gain of Eq. (9) can be arranged as

$$\begin{aligned} g(z) \propto & \\ & g_{1111}(z) + g_{1112}(z) + g_{1121}(z) + g_{1122}(z) + \\ & g_{2211}(z) + g_{2212}(z) + g_{2221}(z) + g_{2222}(z) + \\ & g_{1211}(z) + g_{1212}(z) + g_{1221}(z) + g_{1222}(z) + \\ & g_{2111}(z) + g_{2112}(z) + g_{2121}(z) + g_{2122}(z). \end{aligned} \quad (13)$$

The 1st row of terms contributes only to the growth of the 1st Stokes mode while the 2nd row of terms contributes only to the growth of the 2nd Stokes mode. The remaining two rows are cross terms describing the interaction of the 1st Stokes mode with the 2nd Stokes mode. Since it turns out that the array is symmetric with regards to an interchange of the indices j and v , the 3rd and 4th rows of Eq. (13) are equivalent to one another. It should also be noted that the array is symmetric with regards to an interchange of the indices m and q .

To approximate the gain of the individual modes, this derivation attributes the 3rd row of terms to the growth of the 1st Stokes mode and attributes the 4th row of terms to the growth of the 2nd Stokes mode. Under this assumption, the amplitude of the 1st Stokes mode affects the gain of the 2nd Stokes mode as much as the amplitude of the 2nd Stokes mode affects the gain of the 1st Stokes mode. This approximation tends to equalize the gain of the various modes of the fiber and therefore underestimates the effects of mode competition.

By generalizing this approximation to a fiber with an arbitrary number of modes, the gain given by Eq. (9) can be transformed into the following expression for the Raman gain of the j^{th} mode of a multimode fiber

$$g^j(z) = g_R [\varepsilon_0 \text{cn}(r)]^2 \frac{A_s^j \sum_v A_s^v \sum_m A_p^m \sum_q A_p^q \gamma^{jvmq}}{P_s(z) P_p(z)}. \quad (14)$$

Not only does Eq. (14) consider the interaction of the pump modes with the Stokes modes of the fiber, it also considers how the power in one Stokes mode affects the gain of neighboring Stokes modes. Eq. (14) applies equally to either a forward or a backward propagating Stokes beam. Using Eq. (14), the gain of the modes can be calculated for any input distribution of the pump beam.

Given that spontaneous Raman scattering provided all transverse Stokes modes with equal initial power, the dominant transverse Stokes mode is the mode with the largest Raman gain. Modeling SRS beam cleanup is therefore a matter of determining which Stokes mode of the fiber has the greatest gain. The gain of each mode given by Eq. (14) essentially consists of two parts: the overlap integral, γ^{jvmq} and the mode distribution denoted by the mode amplitudes.

3. Numerical results

3.1 Overlap integrals

We begin by considering the overlap of pure pump modes and pure Stokes modes in a notional fiber, i.e. $j=v$, $m=q$ in Eq. (14). Essentially, this calculation assumes that each Stokes mode interacts with only a single pump mode. The simplified overlap integrals of several lower-order transverse modes of a notional graded-index fiber, presented in Table 1, are normalized to the value of the LP_{01} - LP_{01} overlap. The form of the transverse mode fields of a weakly guiding graded-index fiber is given by Eq. (6). The notional fiber had a 50 μm core ($NA=0.2$). The pump wavelength was 1064 nm and the Stokes wavelength was 1116 nm. The index profile of the fiber was assumed to be $n^2(r) = n_{\text{core}}(1 - 2\Delta r^2)$, where r is the normalized radius; $n_{\text{core}}=1.5$, for the pump and Stokes beams respectively and where

$$\Delta = \frac{1}{2} \left(\frac{NA}{n_{\text{core}}} \right)^2.$$

Table 1 lists the normalized overlap integrals of several pump modes and Stokes modes of a graded-index fiber. The normalized values are given because our purpose is to compare the behavior of the various modes of the fiber. The values in Table 1 show that the overlap of the intensity pattern of the LP_{01} pump mode with the intensity pattern of the LP_{01} Stokes mode (shown in blue) is greater than the overlap of any other pair of intensity patterns. The largest values of the overlap integral occurred when a pump mode overlapped with its corresponding

Stokes mode (i.e., the diagonal elements highlighted in bold). The values in this table are in close agreement with the values reported by Polley and Ralph [9]. Furthermore, the overlap integrals generally became progressively smaller for higher-order transverse modes. According to this simple description, mode competition in a graded-index fiber favors the LP_{01} Stokes mode.

Table 1. This table of the normalized overlap integrals of a graded-index fiber shows that the overlap of the LP_{01} Stokes mode with the LP_{01} pump mode (highlighted in blue) is larger than any other overlap integral. Other self-overlap integrals are highlighted in bold.

		Pump Modes						
		LP_{01}	LP_{11}	LP_{21}	LP_{02}	LP_{31}	LP_{12}	LP_{41}
Stokes Modes	LP_{01}	1.0000	0.5120	0.2622	0.5003	0.1162	0.3781	0.0687
	LP_{11}	0.4880	0.7496	0.3838	0.2562	0.2620	0.3754	0.1677
	LP_{21}	0.2381	0.3658	0.5618	0.2557	0.3197	0.1922	0.2455
	LP_{02}	0.5003	0.2441	0.2437	0.4994	0.2495	0.2619	0.2243
	LP_{31}	0.1162	0.2380	0.3046	0.2495	0.4679	0.1933	0.2795
	LP_{12}	0.3721	0.3754	0.1832	0.2379	0.1813	0.4675	0.1920
	LP_{41}	0.0567	0.1451	0.2230	0.2123	0.2664	0.1976	0.4092

The simplified overlap integrals, ψ^{ijmm} , of several lower-order pure transverse modes of a notional step-index fiber are provided in Table 2. Again, the values of in this table are normalized to the value of the LP_{01} - LP_{01} step-index overlap integral. The mode fields of the step-index fiber are defined by Eq. (7). The notional step-index fiber had a 50 μm core ($NA=0.2$); $n_{\text{core}}=1.5$. The pump wavelength was 1064 nm and the Stokes wavelength was 1116 nm. This table of overlap integrals is similar to the results obtained by Chiang [1]; it should be noted that Chiang ignored the wavelength dependence of the V -number in his analysis, which accounts for the fact that the overlap integrals in Chiang's tables are transposed relative to the diagonal. For example, the overlap of the LP_{01} pump mode with the LP_{11} Stokes mode is equal to the overlap of the LP_{11} pump mode with the LP_{01} Stokes mode. Generally, mode competition in a step-index fiber does not favor the LP_{01} Stokes mode. Instead, in a step-index fiber, the overlap of the higher-order transverse modes with their respective pump modes is greater than the overlap of the LP_{01} Stokes mode with the LP_{01} pump mode. Modes with normalized overlap integrals greater than one have better overlap with their respective pump beam than the overlap of the LP_{01} Stokes mode with the LP_{01} pump mode; the overlap of the LP_{12} Stokes mode with the LP_{12} pump mode has the largest value of all the overlap integrals tabulated in Table 2. This is a stark contrast to the overlap integrals of a notional graded-index fiber tabulated in Table 1.

Table 2. This table of the normalized overlap integrals of a step-index fiber shows that the overlap of the LP_{12} Stokes mode with the LP_{12} pump mode (highlighted in blue) is larger than any other overlap integral. The overlap of the LP_{01} Stokes mode with the LP_{01} pump mode has a lower value than several of the self-overlap integrals highlighted in bold, suggesting that higher-order Stokes modes will dominate the Stokes output.

		Pump Modes						
		LP_{01}	LP_{11}	LP_{21}	LP_{02}	LP_{31}	LP_{12}	LP_{41}
Stokes Modes	LP_{01}	1.0000	0.6683	0.5130	0.8209	0.3749	0.7538	0.2838
	LP_{11}	0.6664	1.0606	0.6772	0.4217	0.5659	0.7391	0.4695
	LP_{21}	0.5094	0.6744	1.1095	0.4106	0.6784	0.3952	0.6029

	LP_{02}	0.8215	0.4208	0.4096	1.1986	0.4044	0.6778	0.3932
	LP_{31}	0.3715	0.5624	0.6770	0.4053	0.9981	0.3489	0.6242
	LP_{12}	0.7540	0.7394	0.3946	0.6737	0.3470	1.2491	0.3343
	LP_{41}	0.2803	0.4651	0.5997	0.3931	0.6223	0.3363	0.9151

A complete explanation of beam cleanup however, requires the mode distribution of the pump beam to be considered in conjunction with the overlap integrals. While the gain of the Stokes modes of a fiber given by Eq. (14) depends on the value of the overlap integral, γ^{jvmq} , the gain also depends on the distribution of the pump beam, $A^m A^q$; this is considered in the next section.

3.2. Quantifying mode competition

The mode distribution of the pump beam strongly determines the mode distribution of the unseeded Stokes output of a multimode fiber. This was experimentally demonstrated by Chiang, who showed that varying the launching conditions of the pump beam changed the intensity patterns of the output Stokes beam generated by unseeded SRS [1]. This experimentally showed that pump launching conditions influenced the dominant Stokes mode; our model is consistent with these observations.

To model SRS fiber beam cleanup, we evaluated the gain of the Stokes modes of both a notional graded-index fiber and a notional step-index fiber for a variety of launching conditions of the pump beam. We calculated the gain of each Stokes mode using Eq. (14). The mode fields of the graded-index and the step-index fibers are given by Eq. (6) and Eq. (7) respectively. Both the notional graded-index fiber and the notional step-index fiber had a core diameter of 50 μm ($NA=0.2$). However, to limit the computation time, each notional fiber contained only 20 transverse modes as opposed to the hundreds of modes contained in a typical 50 μm fiber. The pump wavelength was 1064 nm; the Stokes wavelength was 1116 nm.

The gain of the fiber modes was calculated for 50,000 different random mode configurations of the pump beam. Each pump mode configuration was defined by the relative amplitude and phase of the modes of the pump beam at the input facet of the fiber ($z=0$). For each configuration, the relative amplitude of each pump mode at the input facet of the fiber was determined by a random number generator; i.e., the pump modes had a uniformly random distribution. In order to account for the initial Stokes beam generated by spontaneous Raman scattering, the amplitude of each Stokes mode had a normalized unit value, i.e. the Stokes modes had a uniform distribution. The relative phase of each pump mode and each Stokes mode was determined via a random number generator.

The results of this simulation are given in Fig. 1, which shows the number of times a given Stokes mode had the greatest Raman gain in both a notional graded-index fiber and a notional step-index fiber. (It should be noted that an LP_{lm} mode in which l is odd has two possible orientations; the transpose orientation is denoted by T .) In the case of the graded-index fiber, the LP_{0l} mode had the highest gain for about 25% of the random launching conditions. The two orientations of the LP_{1l} mode each had the greatest gain for about 12% of the random launching conditions in the graded-index fiber. This is consistent with Chiang's observation that the generated Stokes modes of a graded-index fiber could be tailored by carefully aligning the pump beam. Nevertheless, it is clear that given random launching conditions of the pump beam, the LP_{0l} Stokes mode of a graded-index fiber tended to experience greater gain than any other Stokes modes of the graded-index fiber.

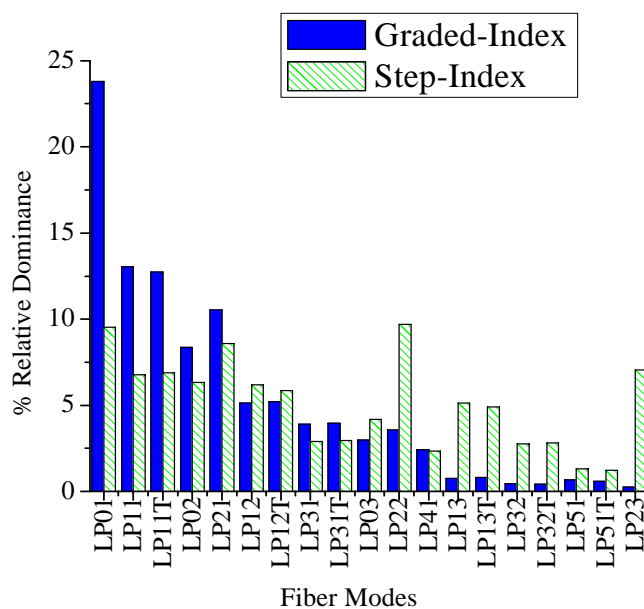


Fig. 1. Probability that a given Stokes mode of a multimode fiber has the greatest Raman gain given random pump launching conditions. In a graded-index fiber, the LP_{0l} mode tends to have much higher gain than the higher-order Stokes modes. In a step-index fiber, the LP_{0l} mode is not dominant; this explains why beam cleanup does not occur in a step-index fiber.

A similar description of SRS beam cleanup is given by Fig. 2, which plots the relative gain of each Stokes mode averaged over each of the 50,000 random pump launching configurations. Again it is clear that in the graded-index fiber the LP_{0l} mode had the greatest average gain; progressively higher-order transverse modes of the graded-index fiber tended to have progressively lower average gain. Clearly the LP_{0l} Stokes mode will experience more gain than the higher-order transverse Stokes modes of a graded-index fiber. In other words, the Stokes beams generated by unseeded SRS in a long fiber will tend to have good beam quality.

Fig. 1 also shows the number of random launching conditions for which the various Stokes modes of a notional step-index fiber had the greatest gain. Generally, the gain of the lower-order transverse Stokes modes of the step-index fiber was similar to the gain of the higher-order transverse Stokes modes of the step-index fiber. A similar description is given by Fig. 2, which plots the gain of each Stokes mode averaged over each of the 50,000 random pump launching configurations. Given a uniform random mode distribution of the pump beam, the LP_{0l} Stokes mode of the step-index fiber did not tend to experience greater gain than several other Stokes modes of the notional step-index fiber. Instead, the gains of several of the Stokes modes of a notional step-index fiber were fairly similar. This shows a sharp contrast between the properties of a graded-index fiber and a step-index fiber; the former exhibits SRS beam cleanup, while the latter does not.

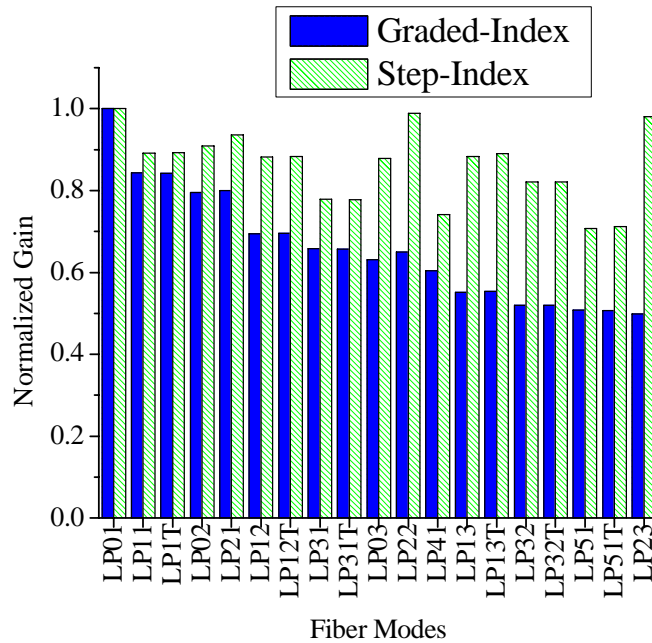


Fig. 2. Average relative gain of various Stokes modes in a multimode fiber calculated for the case of unseeded SRS given 50,000 different sets of random launching conditions of the pump. The LP_{01} Stokes mode of the graded-index fiber has more gain than the higher-order Stokes modes, while the LP_{01} Stokes mode does not have the greatest gain in a step-index fiber. This explains why beam cleanup requires a graded-index fiber.

4. Discussion

To explain the consequences of these formulas, we have produced several graphs of mode configurations in a notional graded-index fiber and in a notional step-index fiber. In Fig. 3, we compare and contrast mode competition in a graded-index fiber to mode competition in a step-index fiber. An exemplary initial pump condition was selected from randomly generated mode configurations of pump beams and applied to both the graded-index and step-index fibers. The pump beam in each fiber had the same number and types of modes with the same relative amplitudes and phases. The initial pump configurations result in different power distributions due to the inherent differences between the two types of fibers. The gain of each Stokes mode, relative to the gain of the LP_{01} mode, was calculated using Eq. (14). The ratio of the growth of the LP_{01} Stokes mode to the growth of the j^{th} Stokes mode was $g_{relative} = \exp(g^l/g^j)$; furthermore, pump depletion was ignored.

The Stokes beam resulting from propagation down a long length of graded-index fiber, given the pump configuration of Fig. 3(a), is shown in Fig. 3(b). The evolution of the Stokes beam in this notional graded-index fiber is shown in the animation of Fig. 4. The first frame of the animation, which shows the Stokes beam generated by spontaneous Raman scattering, resulted from the initial condition that each Stokes mode contained equal power. Each subsequent frame shows the evolution of the Stokes beam as each mode in the previous frame was amplified by a factor of $g_{relative}$. As shown in Fig. 1 and Fig. 2, the output Stokes configuration is highly dependent on the pump condition. A different set of pump conditions would result in a different output Stokes configuration than shown in the animation. However, Fig. 1 and Fig. 2 show that the dominant Stokes mode shown in the animation tends to be the preferred Stokes output configuration generated by a graded-index fiber.

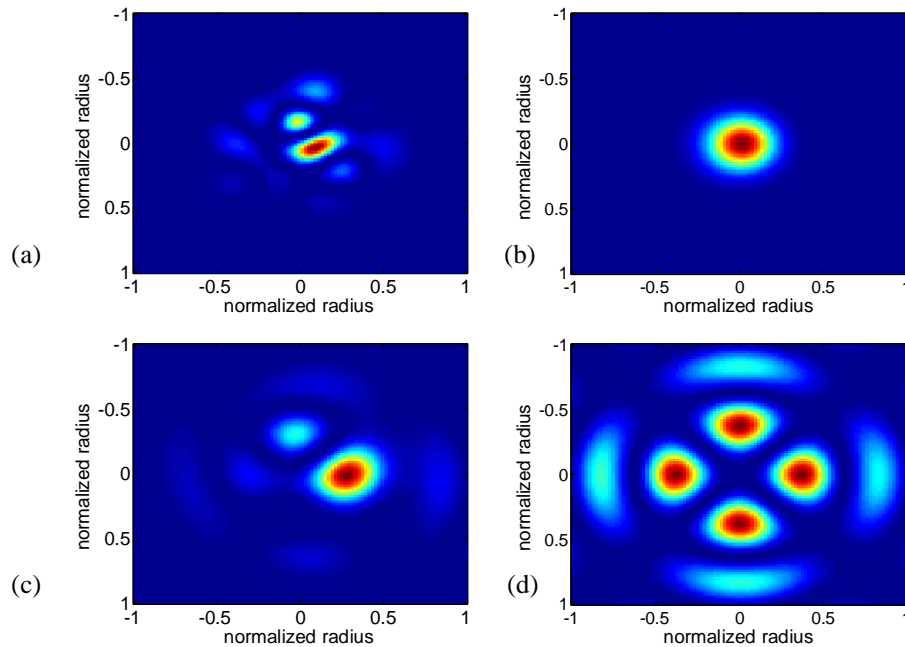


Fig. 3. A comparison of mode competition in a graded-index fiber and a step-index fiber. In a notional graded-index fiber, the pump configuration shown in (a) resulted in the Stokes output shown in (b). In a notional step-index fiber, the pump configuration shown in (c) resulted in the Stokes output shown in (d).

By contrast, this same random pump configuration for a step-index fiber is shown in Fig. 3(c). The Stokes output resulting from the pump configuration of Fig. 3(c) is shown in Fig. 3(d). The evolution of the Stokes modes in the notional step-index fiber is depicted in the animation of Fig. 5. In the first frame of the animation, which shows the initial Stokes beam generated by spontaneous Raman scattering, each Stokes mode contained an equal amount of power. Each subsequent frame shows the Stokes beam as each mode in the previous frame was amplified by a factor of g_{relative} . Even though the notional step-index fiber uses the same pump configuration as the graded-index fiber, the Stokes output was very different. It should be noted that a different pump configuration will correspond to a different Stokes evolution. However, as shown in Fig. 1 and Fig. 2, the lower-order Stokes modes will not tend to dominate the Stokes output of a step-index fiber.

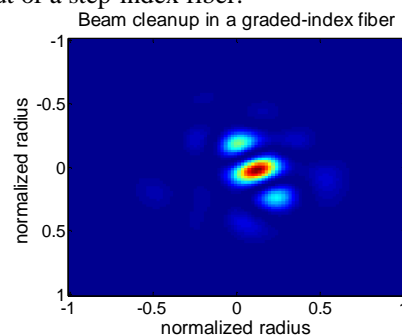


Fig. 4. An animation depicting SRS beam cleanup in a graded-index fiber. The Stokes beam generated by spontaneous Raman scattering in a graded-index fiber is shown in the first frame. Subsequent frames show the evolution of the Stokes beam as each Stokes mode is amplified by g_{relative} . (MOV video, Figure4.mov, 0.7 Mbytes).

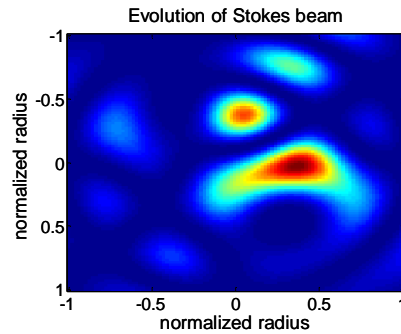


Fig. 5. An animation depicting the Stokes evolution associated with SRS in a step-index fiber. The Stokes beam generated by spontaneous Raman scattering in a step-index fiber is shown in the first frame. Subsequent frames show the evolution of the Stokes beam as each Stokes mode is amplified by $g_{relative}$. (MOV video, Figure5.mov, 1.0 Mbytes).

5. Conclusion

This model explains how mode competition in a graded-index fiber leads to SRS fiber beam cleanup. The lower-order transverse modes of a graded-index fiber tend to have good overlap with the pump modes of the fiber, while the higher-order transverse Stokes modes have a poor overlap with the pump modes. As a result, the lower-order Stokes modes of a graded-index fiber experience more gain than the higher-order Stokes modes of the fiber and the lower-order transverse Stokes modes dominate the Stokes output. Thus, a multimode pump beam in a graded-index fiber can be used to generate a Stokes beam which is near-singlemode. Furthermore, this model shows that the dominant mode of the Stokes beam can be made to propagate in various lower-order transverse modes of the fiber by adjusting the launching conditions of the pump beam. This is consistent with experimental observations reported by Chiang [1].

We also examined the overlap of the pump and Stokes modes of a notional step-index fiber. The overlap of the lower-order transverse Stokes modes with the pump modes was similar to the overlap of the high-order transverse modes with the pump modes. As a result, the LP_{01} Stokes mode was not the dominant component of the Stokes output. Instead, the gain of the lower-order transverse Stokes modes was shown to be similar to the gain of several of the higher-order transverse Stokes modes. This explains why the SRS beam cleanup effect has not been observed in step-index fibers [9,10].